Case Studies in Thermal Engineering 26 (2021) 101156

Contents lists available at ScienceDirect

Case Studies in Thermal Engineering

journal homepage: www.elsevier.com/locate/csite

Evaluation of the energy storage performance of PCM nano-emulsion in a small tubular heat exchanger

Liu Liu [a], Jing Li [a,1], Jianlei Niu [b], Jian-Yong Wu [a,*]

[a] Department of Applied Biology & Chemical Technology, The Hong Kong Polytechnic University, Hung Hom, Kowloon, Hong Kong
[b] Department of Building Services Engineering, The Hong Kong Polytechnic University, Hung Hom, Kowloon, Hong Kong

ARTICLE INFO

Keywords:
PCM emulsion
Cooling energy storage
Tubular heat exchanger
Charging and discharging rate
Thermal storage capacity

ABSTRACT

PCM emulsions have attracted considerable interest as the media for thermal energy storage (TES) owing to their high thermal storage capacity, desirable fluidity and thermal conductivity. However, the direct transportation of PCM emulsions in TES systems for both charging and discharging is rarely reported. In this work, a PCM-in-water nano-emulsion was prepared with *n*-hexadecane and suitable surfactants for cooling energy storage at a charging and discharging temperature range of 20–5 °C and 5–15 °C, respectively. It was applied to a tubular heat exchanger system to evaluate its TES performance for a cooling panel of 0.2 m^2 total surface area. The thermal storage performance was notably increased with the flow rate of emulsion through the exchanger tube. The volumetric thermal storage capacity of charging was 50% higher than that of water. The cooling energy could be rapidly released in the discharging process, 79% of the stored energy at averaging 25 W during most of the discharging period. The emulsion remained stable throughout the test period. Overall, the results demonstrated that the PCM nano-emulsion has the unique characteristics of high static stability, and high energy releasing efficiency and the promising potential for air-conditioning application in buildings.

1. Introduction

The rapid consumption of fossil fuels for energy generation is mainly responsible for the rising atmospheric carbon dioxide content, global warming and the worsening environment pollution. There is an urgent call for the use of clean and renewable energy resources such as wind and solar energy. However, the energy supply from the renewable sources is strongly affected by the mismatch with the demand and the variation with time and location. Thermal energy storage (TES) technologies have been developed to overcome these problems. Compared with other TES systems, the latent heat storage systems using phase change materials (PCMs) have the advantages of high energy storage density, chemical stability and flexible working temperatures [1,2]. However, the heat transfer rate of TES systems with PCMs is relatively low due mainly to the low thermal conductivities of PCMs (0.2–0.5 W/m·K) [3]. Considerable effort has been made to developing various forms of PCMs such as shape-stabilized PCM [4], nano-enhanced PCM [5], and micro-encapsulated PCM (MPCM) [6] for heat transfer enhancement. The issue has also been addressed through analysis of the relationships between the heat transfer and storage capacity of TES systems. Fang et al. [7] proposed the effective storage ratio (E_{st}) and capacity effectiveness (ϕ) as indicators for the practical performance of a shell-and-tube energy storage unit. In the laminar region of a heat

* Corresponding author.
E-mail address: Jian-yong.wu@polyu.edu.hk (J.-Y. Wu).
[1] Jing Li current affiliation: Shaanxi Institute of Metrology Science, Xi'an, China.

https://doi.org/10.1016/j.csite.2021.101156
Received 26 March 2021; Received in revised form 5 June 2021; Accepted 11 June 2021
Available online 13 June 2021

Nomenclature

C_p	Specific heat capacity, kJ/(kg·°C)
ΔE	Cooling energy storage, J
E_V	Volumetric thermal storage capacity, J/m^3
H	Latent heat, kJ/kg
$\dot{m}$	Mass flow rate, kg/s
Q	Energy, J
ΔQ	Energy difference, J
q	Charging/discharging rate, W
R	Thermal resistance, °C/W
T	Temperature, °C
ΔT	Temperature difference, °C
V	Volume, m^3

Greek symbols

τ	Time, s

Subscripts

avg	Average
c	Charging
d	Discharging
e	End
eff	Effective heat capacity
emu	PCM nano-emulsion
i	Initial
in	Inlet
lab	Laboratory
loss	Heat loss
m	Melting
out	Outlet
t	Tank
w	Water

transfer fluid with a high thermal conductivity of nano-enhanced PCM (20 W/m·K), E_{st} is about 2 and ϕ is in the range of 80–90%. As the Reynolds number increases, both E_{st} and ϕ decrease dramatically, indicating that the TES unit cannot effectively release the stored energy, which limits its application for fast energy release situations. To overcome this drawback, thermal storage media in fluid form have been proposed, such as MPCM slurries and PCM emulsions [8], which act as the heat transfer fluid and the thermal storage media simultaneously. Several recent studies have evaluated the thermo-fluidic characteristics of thermal storage fluids [8–11]. Their potential advantages include easier transportation in pipes, higher storage capacity in comparison to water (1.5–2 times), and more efficient heat transfer, and faster energy release and overall, a higher high effectiveness. Such a TES system is also simple to construct and easy to control and operate.

Diaconu et al. [12] investigated the natural convection heat transfer of MPM slurry and water in a tank containing a helically coiled heating tube, where the MPM slurry significantly enhanced the heat transfer coefficient during phase change, up to 5 times higher than that of water. Huang et al. [13] studied the MPM slurry from a commercial supplier BASF at 25%, 35% and 50% mass concentrations in a TES system consisting of a helical coil heat exchanger but found that the 50% MPCM slurry was not feasible because of high viscosity and low thermal conductivity. Zhang and Niu [14] experimentally investigated two key thermal storage parameters, discharging rate and volumetric thermal storage capacity of a MPCM slurry in a coil heat exchanger tank for heating or cooling. The volumetric thermal storage capacity of the MPCM slurry was nearly two-fold higher than that of water in the range of 8–18 °C, but its discharging rate was much lower. Xu et al. [15] also studied the charging rate and heat transfer coefficient of a MPCM slurry in a similar TES system but found no obvious improvement of the charging rate or heat transfer coefficient in comparison to water during the whole charging process. In most of these previous studies, the MPCM slurries were placed in tanks on the outside of heat exchanger coils rather than flowing inside the pipe for charging or discharging, which is unfavorable for the development of thermal storage fluids. This is most possibly caused by the breakage of a hard polymer shell during the fluid transportation by pumps or sedimentation of solid MPCM particles, leading to lower efficiency or even pipeline blockage.

As a result, the PCM emulsions have been developed as a new class of thermal storage fluids. Compared to the larger MPCM slurries, PCM emulsions with small droplets surrounded by a flexible and protective surfactant layer can be more easily transported through the pipes and pumps, without the probability of shell breakage or pipeline blockage. Moreover, PCM nano-emulsions with very small droplet size can further increase the stability and are even more favorable for an efficient TES system. Ma et al. [16] studied the thermo-fluidic performance of 10 and 20 wt% PCM emulsions of 290 nm average droplet size in tubes of 2 and 4 mm inside diameters

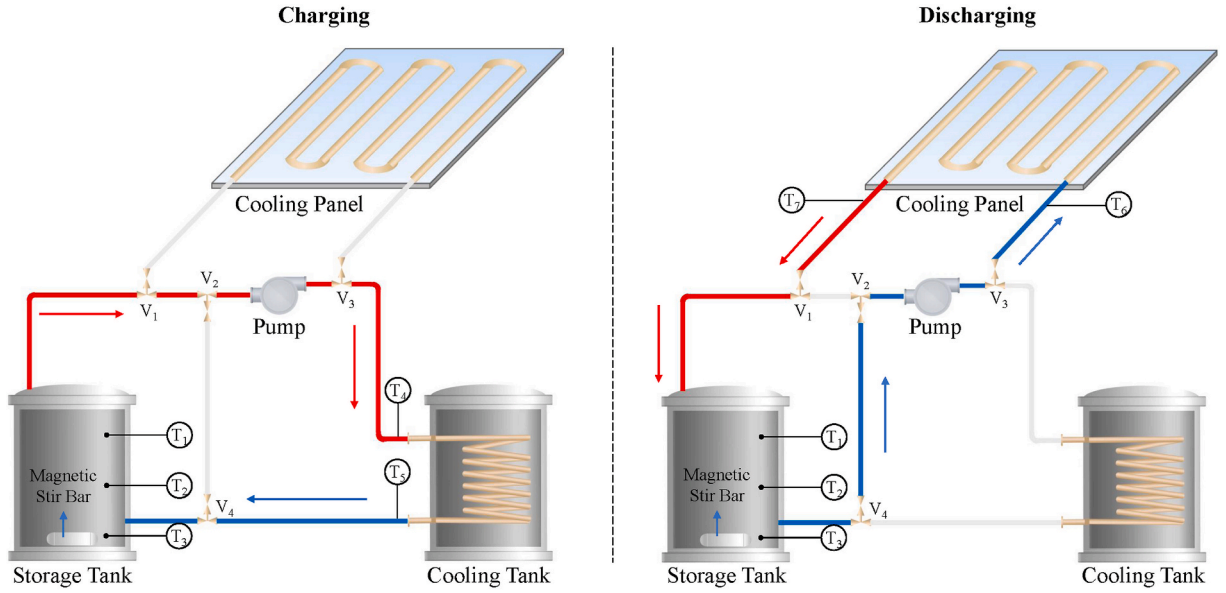

Fig. 1. The schematic diagram of experimental rig. By controlling four three-way valves (V_1–V_4), PCM nano-emulsion in the storage tank was directly pumped to the cooling tank or cooling panel, referring to the charging or discharging process.

(ID) in a laminar flow. Morimoto and Kumano [17,18] experimentally studied the flow and heat transfer characteristics of 10–30 wt% *n*-hexadecane and *n*-octadecane emulsions of droplet size 200–400 nm in a 1-m long and 7.5 mm ID tube in both laminar and turbulent flow. Delgado et al. [19] experimentally investigated the volumetric thermal storage capacity and heat transfer rate of a low-cost PCM emulsion in a 46 L tank with a helical-coil heat exchanger. Their results showed that the volumetric thermal storage capacity of PCM emulsion was 34% higher than with water, though the overall heat transfer coefficient was much lower. A later study from the same group in a stirred tank [20] showed that the overall heat transfer coefficient was 3.5–5.5 times higher than that of water at 290–600 rpm stirring speeds. However, these reported PCM emulsions were also placed in the tank due probably to a poor stability with a larger droplet size.

To the best of our knowledge, there is still no reported study on the performance of PCM nano-emulsions flowing through tubular TES systems for the charging and discharging process. Therefore, this work aims to test the TES performance of a PCM nano-emulsion with a droplet size below 100 nm for cooling energy storage in a self-designed small-scale tubular heat exchanger system. Firstly, a highly stable *n*-hexadecane-in-water nano-emulsion of was prepared based on an optimized recipe. The thermal storage characteristics of the emulsion including the volumetric thermal storage capacity and charging and discharging rate were evaluated at various flow rates through the tube and stirring speeds in the storage tank during the charging and discharging processes.

2. Materials and experimental setup

2.1. Preparation of PCM nano-emulsion

The PCM nano-emulsion for this study was prepared with the phase inversion temperature (PIT) method as reported previously [21]. It consisted of 20% *n*-hexadecane, 9.5% of a surfactant mixture of Brij L4 and polyethylene-*block*-(ethylene glycol) at 7:2.5 mass ratio and 1.5% *n*-tetracosane (all in weight%). The PCM component *n*-hexadecane had an onset melting temperature of about 17 °C and a latent heat of 245 kJ/kg. The nucleating agent used in the previous study, *n*-octacosane, was replaced with *n*-tetracosane in order to achieve a lower degree of supercooling without costing the stability of the nano-emulsion.

The droplet size of emulsion was measured by dynamic light scattering (Malvern Zetasizer Nano ZS) and thermal properties determined with a differential scanning calorimeter (Mettler Toledo, DSC3). The apparent viscosity was measured with a rotational viscometer using the ultra-low viscosity adapter (Brookfield, DV3T).

2.2. Experimental setup and conditions

A self-designed small-scale tubular heat exchanger system was constructed to test the charging and discharging performance of the PCM nano-emulsion as illustrated schematically in Fig. 1. It consisted of a storage tank, a cooling tank, a cooling panel, a metering pump and four three-way valves which were connected with plastic tubing (5 mm of inside diameter). The tubing and the storage tank were insulated with a layer of 10 mm high-density polyurethane foam. The storage tank had an inside diameter of 110 mm and a height of 145 mm (internal volume ~1.3 L) with a magnetic stirrer for agitation. The cooling tank was a thermal flask with a double stainless-steel wall and an internal volume of 1.5 L filling which was filled with ice slurries. A helical coil of copper tube of 6 mm inside diameter

and 2 m total length was enclosed inside the cooling tank. The air-cooling panel was made of 6 mm inside diameter with a total length of 2.5 m, which was fixed on a steel sheet of 0.2 m^2. Room temperature during the test was controlled at 23.0 ± 0.5 °C.

A diaphragm metering pump with an accuracy of 2% of the flow rate was installed to control and measure the flow rate of emulsion. Seven T-type thermocouples with an accuracy of ±0.2 °C were instilled in the system, three (T_1-T_3) of which were used to detect the emulsion temperature from the top to the bottom of the storage tank. The other four thermocouples were attached to the surface of copper tube to measure the inlet and outlet temperature of PCM nano-emulsion passing through the cooling tank (T_4-T_5) or cooling panel (T_6-T_7). A data acquisition unit was used to collect the temperature data at a time interval of 1 s.

Both charging and discharging processes could be operated in the system by controlling four three-way valves (V_1–V_4). During the charging process, the path to the cooling panel was closed by adjusting V_1 and V_3, and the connection between V_2 and V_4 was stopped. The metering pump was switched on to transport the PCM nano-emulsion from the top layer of the storage tank through V_1–V_2–V_3 to the cooling tank; then cooled emulsion flew through V_4 back to the bottom of the storage tank. The flow rate of PCM emulsion through the system and the agitation speed in the storage tank were varied to evaluate their effects on the charging rate and the volumetric thermal storage capacity. During the discharging process, the path to the cooling tank was closed by adjusting V_3 and V_4, and connection between V_1 and V_2 was stopped. The cold PCM nano-emulsion was pumped from the bottom of the storage tank to the cooling panel through V_4–V_2–V_3; the heat-exchanged emulsion was returned to the top of storage tank through V_1. Various flow rates were tested at a constant stirring speed to evaluate the discharging performance. The total volume of PCM nano-emulsion was about 1.2 L.

3. Thermal analysis methods

During a time period from τ_i to τ_e of the charging process, the cooling energy storage in PCM nano-emulsion ΔE_{emu} is represented by,

$$\Delta E_{emu} = m_{emu} C_{p,eff} \, (T_e - T_i) \tag{1}$$

where m_{emu} is the mass of PCM nano-emulsion in the storage tank, T_e and T_i are the end and initial emulsion temperature, respectively, and $C_{p,eff}$ is the effective specific heat capacity as defined by Ref. [22],

$$C_{p,eff} = \begin{cases} C_{p,emu} & if\ T_{emu} > T_m\ or\ < T_m \\ C_{p,emu} + H/\Delta T & if\ T_{emu} = T_m \end{cases} \tag{2}$$

where $C_{p,emu}$ is the heat capacity and H the latent heat of PCM nano-emulsion, and ΔT is the melting or freezing temperature range.

During a time period from τ_i to τ_e of the discharging process, the cooling energy released by the cooling panel Q_d is given by,

$$Q_d = \int_{\tau_i}^{\tau_e} \dot{m} C_{p,eff} \, (T_{out} - T_{in}) d\tau = \int_{\tau_i}^{\tau_e} \dot{m} C_{p,eff} \, (T_7 - T_6) d\tau \tag{3}$$

where $\dot{m}$ is the mass flow rate of PCM nano-emulsion, T_6 and T_7 are the emulsion temperatures at the cooling panel inlet and outlet, respectively.

Both charging and discharging rates, q, can be calculated by,

$$q = \dot{m} C_{p,eff} \, |T_{out} - T_{in}| \tag{4}$$

At a specific temperature range, the volumetric thermal storage capacity of the charging process ($E_{V,c}$) and discharging process ($E_{V,d}$) can be obtained from the following equations,

$$E_{V,c} = \frac{\Delta E_{emu}}{V_{emu}} = \frac{m_{emu} C_{p,eff} \, (T_e - T_i)}{V_{emu}} \tag{5}$$

$$E_{V,d} = \frac{Q_d}{V_{emu}} = \frac{\int_{\tau_i}^{\tau_e} \dot{m} C_{p,eff} \, (T_7 - T_6) d\tau}{V_{emu}} \tag{6}$$

The overall uncertainty of the experimental results, δR, is associated with various independent factors (X_1, X_2, …, X_n); δX_n is the measurement error of each factor as give by Ref. [23],

$$\delta R = \sqrt{\sum_{n=1}^{N} \left(\frac{\partial R}{\partial X_n} \delta X_n \right)^2} \tag{7}$$

In the present study, the uncertainty analysis was performed for the charging/discharging rate (q) and the volumetric thermal storage capacity (E_V) derived from the measurement accuracy of the volume flow rate, temperature difference and volume. The accuracy of volume measurement was 1%. Therefore, the maximum uncertainties of q_c and $E_{V,c}$ were 8.25% and 3.48%, respectively, while the maximum uncertainty values of q_d and $E_{V,d}$ were 20.1% and 20.12%, respectively.

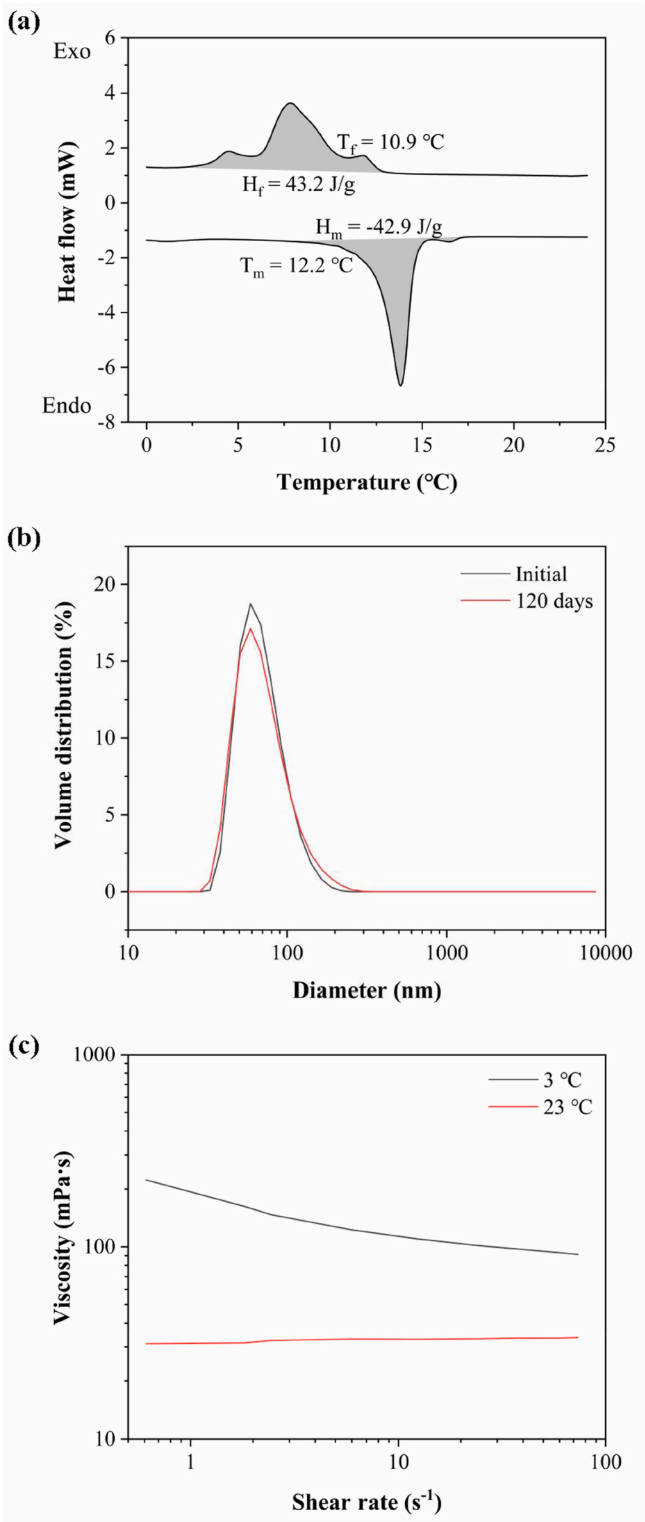

Fig. 2. Characteristics of 20 wt% *n*-hexadecane nano-emulsion: (a) DSC curves; (b) droplet size distribution upon preparation and after 120 days; (c) apparent viscosity-shear rate curves at 3 and 23 °C.

Table 1
The effective specific heat capacity ($C_{p,eff}$) of PCM nano-emulsion with different melting and freezing temperature range.

Process	Temperature (°C)	$C_{p,eff}$ (kJ/(kg·°C))
Melting	>15 or <12	3.7
	12–15	18.0
Freezing	>11 or <6	3.7
	6–11	12.3

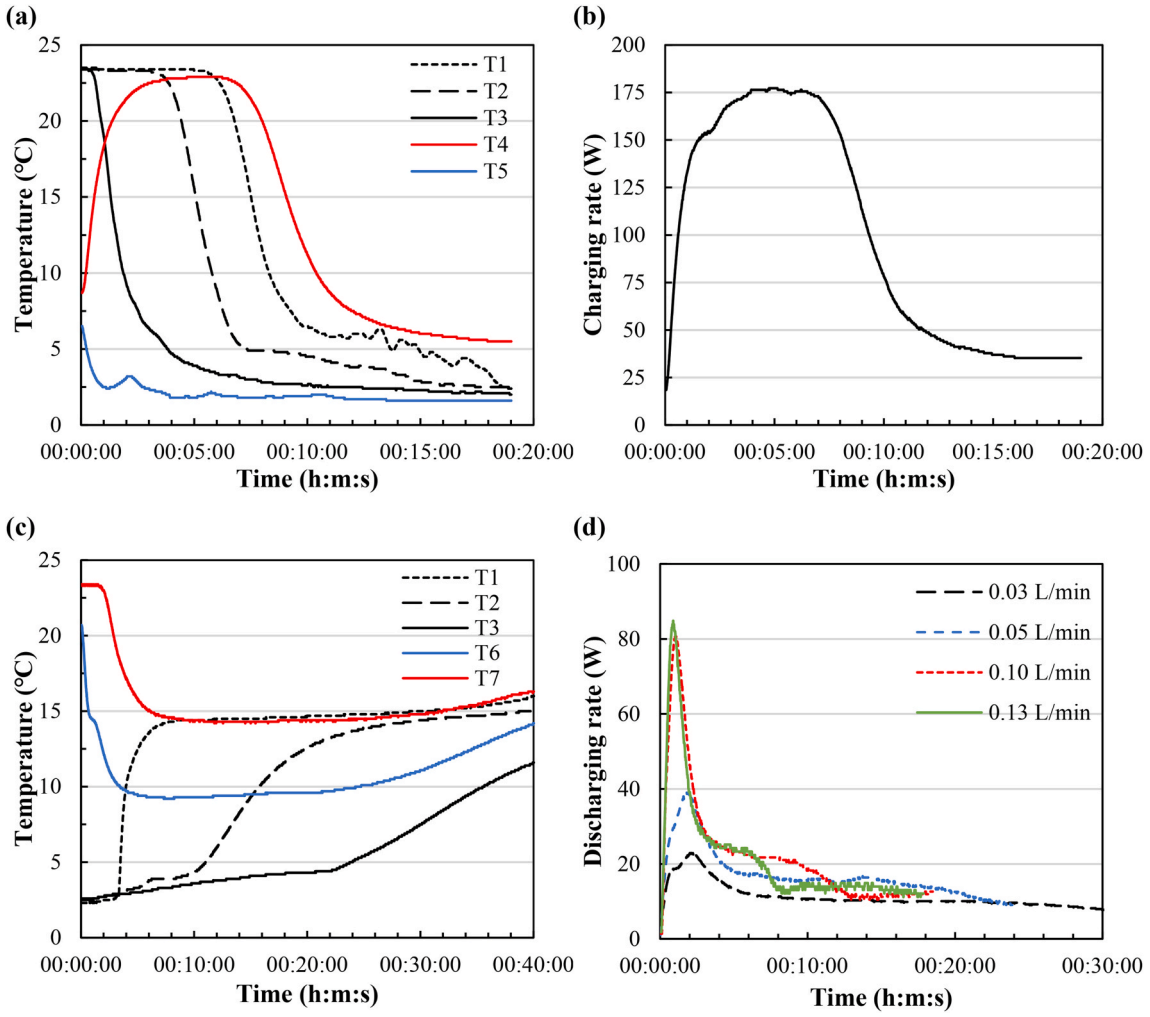

Fig. 3. The charging and discharging processes when water was used as the medium: (a) charging process at flow rate of 0.12 L/min and no stirring in the storage tank; (b) charging rate curve; (c) discharging process at flow rate of 0.03 L/min and no stirring in the storage tank; (d) discharging rate curves at different flow rates (0.03–0.13 L/min).

4. Results and discussion

4.1. Properties of PCM nano-emulsions

Fig. 2 shows the major properties of *n*-hexadecane nano-emulsion including the droplet size, viscosity and thermal properties. As shown in Fig. 2a, the emulsion had an onset melting and freezing point 12.2 and 10.9 °C, respectively, giving a supercooling degree of 1.3 °C. The melting and freezing temperature range were 3 and 5 °C, respectively, resulting in the $C_{p,eff}$ difference of the emulsion melting and freezing, as shown in Table 1. In addition, cooling of the emulsion to around 5 °C would lead to the full crystallization of *n*-hexadecane nano-droplets. The latent heats of melting and freezing were almost equal of about 43.0 kJ/kg. The *n*-hexadecane nano-

Table 2
Comparison of cooling energy release through cooling panel at different flow rates.

Flow rate (L/min)	0.03	0.05	0.10	0.13
Cooling energy (kJ)	21.1	24.4	24.8	23.3

emulsion showed a high stability for over 120 days with a minor change in the droplet size, from 82.0 to 87.1 nm, showing in Fig. 2b. At room temperature, the apparent viscosity was nearly unchanged (~32 mPa s) with the increasing shear rate, indicating a Newtonian fluid behavior. However, when the *n*-hexadecane nano-droplets were completely solidified at a low temperature, the emulsion exhibited a similar shear-thinning characteristic of a pseudoplastic fluid with the apparent viscosity decreasing with shear rate. As shown in Fig. 2c, at shear rate of 0.6 s^{-1}, the apparent viscosity was over 200 mPa s. Since the designed volumetric flow rate was very small, the pressure drop and pumping power consumption were not much different from those with water. In addition, the flow of emulsion through the tube and coil was laminar at all tested flow rates with Reynolds number no more than 100. The density and specific heat capacity were 960 kg/m^3 and 3.7 kJ/(kg·°C), respectively.

4.2. Heat balance analysis

Water as a conventional energy storage fluid was firstly used in the system, not only for calibration of the heat balance, but also for comparison with PCM nano-emulsion. About 1 kg water in the storage tank was pumped at 0.12 L/min and cooled to 2.7 °C, and then kept in the laboratory for 2.5 h, where room temperature was around 23.0 °C, the end temperature of water was raised to 10.0 °C. The total thermal resistance of the storage tank R_t was calculated by the below equation [24] as 4.93 °C/W.

$$R_t = \frac{\left(T_{lab,avg} - T_{t,avg}\right)\tau}{Q_{t,loss}} = \frac{\left(T_{lab,avg} - T_{t,avg}\right)\tau}{m_w C_{p,w}\left(T_{e,w} - T_{i,w}\right)} \tag{8}$$

where $T_{lab,avg}$ and $T_{t,avg}$ are the average temperature of the lab and that of the storage tank during τ period, m_w and $C_{p,w}$ the mass and specific heat capacity of water, $T_{e,w}$ and $T_{i,w}$ the end and initial water temperature in the storage tank, respectively. The corresponding heat balance of charging was estimated by,

$$\Delta Q = Q_c - \Delta E_w - Q_{t,loss} \tag{9}$$

where ΔE_w is the cooling energy storage in water during the charging period, $Q_{t,loss}$ the heat loss of the storage tank, Q_c the cooling energy obtained through the cooling tank from τ_i to τ_e, which is given by,

$$Q_c = \int_{\tau_i}^{\tau_e} \dot{m}_w C_{p,w}\left(T_4 - T_5\right) d\tau \tag{10}$$

The difference ΔQ is equivalent to the error of heat balance, and $\Delta Q/Q_c$ was calculated as 20.8%. This large relative error could be attributed to the following three causes. Firstly, the inlet and outlet temperatures of the cooling tank (T_4 and T_5) were measured at the surface of the copper tube rather than the inside fluid temperature, which would cause error for Q_c calculation, especially at a low fluid temperature that was more easily affecting by the environment. Secondly, other components such as the storage tank would store cooling energy. The third was the heat loss of plastic tubing, which was not included in Eq. (9). Considering the significant error of the system, Eq. (5) was used to calculate the charging volumetric thermal storage capacity.

4.3. Charging and discharging performance of water

Fig. 3 shows the charging and discharging performance of water at various flow rates without stirring in the storage tank. As shown in Fig. 3a, at the initial stage of charging process, the inlet temperature T_4 quickly increased to the relative level of initial water temperature while the outlet temperature T_5 decreased. The temperature gradient in the storage tank was obvious without stirring, and the water was cooled from the bottom to the top. At the end charging stage, the inlet temperature T_4 was 2–3 °C higher than the cooled water, indicating the considerable heat loss through the plastic tubing. The difference between T_4 and T_5 was increased with time and reached the maximum of 20 °C in about 2 min, as a result of the maximal charging rate as shown in Fig. 3b. The instantaneous charging rate was increased rapidly from 20 to 175 W and stayed for about 5 min. As the top layer started to cool, the inlet temperature T_4 decreased sharply, leading to the sudden decrease of the charging rate.

In the discharging process, the temperature distribution of the storage tank was presented in Fig. 3c. Conversely, the temperature in storage tank started to rise from the top to the bottom. The difference between the inlet and outlet temperature of cooling panel (T_6 and T_7) remained at around 5 °C. Fig. 3d displays the discharging rate of water, calculated by Eq. (4), at flow rates from 0.03 to 0.13 L/min. At the initial discharging stage, the instantaneous discharging rate was sharply increased due to the short time intervals for cooled water circulating to the outlet of cooling panel. When the flow rate was high, the time interval was short and the inlet temperature of T_6 was low. The temperature difference of T_6 and T_7 was large in a short period resulting in a dramatic increase of the discharging rate. After the initial stage, discharging rate was decreased, and it can be seen that the higher flow rate of 0.13 L/min remaining at a relative

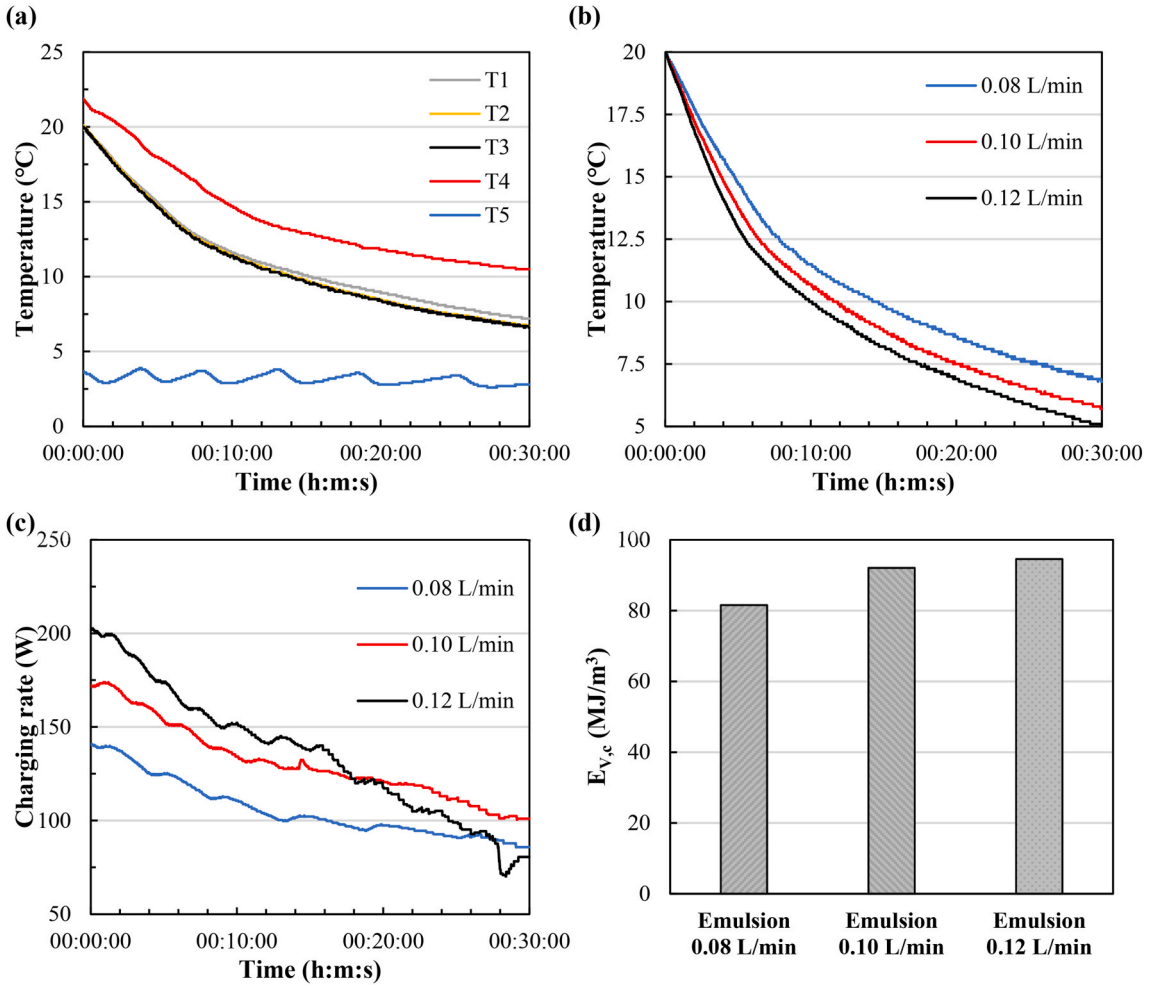

Fig. 4. The charging process of PCM nano-emulsion with different flow rates at 1100 rpm stirring: (a) temperature variations at flow rate of 0.08 L/min; (b) average medium temperature in the storage tank; (c) charging rate curves; (d) volumetric thermal storage capacity.

discharging rate as that of 0.10 L/min for a shorter time. The cooling energy was calculated as given in Table 2. As the flow rate was increased, the cooling energy released by the cooling panel gradually increased to 24.8 kJ at 0.10 L/min. Further increase of the flow rate to 0.13 L/min led to a drop of cooling energy release, suggesting that the cooling capacity of the cooling panel reached the maximum at a flow rate around 0.10 L/min and had no further increase at a higher flow rate.

The above results indicated that the large temperature gradient in the unstirred water storage tank may become more significant with the PCM nano-emulsion with a higher viscosity, which may have a negative effect on the charging performance. Therefore, stirring was applied in the following experiments with the PCM nano-emulsion.

4.4. Charging performance of PCM nano-emulsion

4.4.1. Effect of flow rate

Fig. 4 shows the test results of PCM nano-emulsion at different volumetric flow rates and a fixed stirring speed in the storage tank. Fig. 4a shows the temperature variations in 30 min charging at flow rate of 0.08 L/min. The outlet temperature of cooling tank T_5 flocculated in a narrow range below 4 °C, while the inlet temperature T_4 gradually decreased as the temperature of storage tank was declining. The temperature gradient in the storage tank was negligible except for a slightly higher temperature in the top layer (T_1). The crystallization temperature of PCM nano-emulsion led to a notable slowdown of temperature decrease starting from the range of 11–12 °C, which was consistent with the DSC result. The average temperature of PCM nano-emulsion in 30 min charging at various flow rates was given in Fig. 4b. The temperature drop was faster at a higher flow rate due to the enhanced heat transfer. As a result, the temperature of PCM nano-emulsion dropped to 5 °C at 0.12 L/min, while the corresponding charging end temperatures at 0.08 and 0.10 L/min were 6.9 and 5.7 °C, respectively.

Fig. 4c shows the charging rate of PCM nano-emulsion versus time at various flow rates, derived from Eq. (4). The charging rate

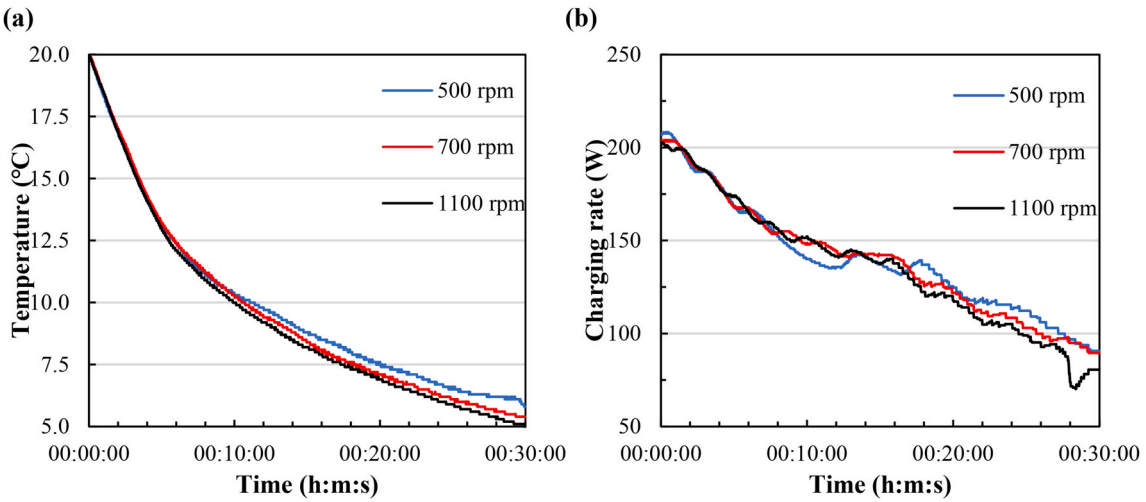

Fig. 5. The charging process of PCM nano-emulsion with different stirring speed at 0.12 L/min: (a) average emulsion temperature in the storage tank; (b) charging rate curves.

Table 3
Comparison of volumetric thermal storage capacity of PCM nano-emulsion under different charging conditions and water in temperature range of 5–20 °C.

	Flow rate (L/min)	Stirring (rpm)	E_V (MJ/m^3)	E_V over water
PCM nano-emulsion	0.08	1100	81.56	1.29
	0.10	1100	92.07	1.46
	0.12	1100	94.56	1.50
	0.12	700	93.14	1.48
	0.12	500	91.72	1.46
Water	0.12	0	63	1

decreased with the decreasing difference, ($T_4 - T_5$) Specifically, the initial charging rate was over 200 W at 0.12 L/min, which was higher than that of water, implying that faster charging can be achieved in the system. However, the charging rate at 0.12 L/min experienced a faster decrease to below that of 0.10 L/min in about 18 min and that at 0.08 L/min at the end charging period (27 min). The charging rate followed a similar trend at 0.08 L/min and 0.10 L/min, and the value at 0.10 L/min was 20–30 W, higher than that of 0.08 L/min throughout the charging period.

Fig. 4d shows the volumetric thermal storage capacity of PCM nano-emulsion ($E_{V,c}$) after 30 min of charging at 0.08–0.12 L/min, derived from Eq. (5). Since the initial temperature was all at 20 °C, a higher flow rate led to a lower end temperature during the same period, and hence a higher $E_{V,c}$. Consequently, the volumetric thermal storage capacity was 94.56 MJ/m^3 at 0.12 L/min, about 16% higher than 81.56 MJ/m^3 at 0.08 L/min. The above results demonstrated that the higher flow rate of PCM nano-emulsion during the charging process was more efficient for the system.

4.4.2. Effect of stirring in the storage tank

Fig. 5 shows the test results of PCM nano-emulsion at a fixed flow rate and various stirring speeds in the storage tank. Above the onset freezing temperature, the average temperature of emulsion in the storage tank decreased rapidly and the stirring speed had negligible influence on the heat transfer performance (Fig. 5a). When the emulsion began to freeze, the effect of stirring appeared with a slower temperature drop at a higher stirring speed. After 30 min of charging, the end cooling temperature was 5.9 °C and 5.4 °C for 500 rpm and 700 rpm, respectively. Compared with the flow rate, the stirring speed had a smaller effect on the charging performance, due mostly to the direct transportation of PCM nano-emulsion for cooling. Many other reported TES systems [14,20] were equipped with heat exchanger units that were immersed in a PCM storage tank for the cooling of water by PCM-based fluids such as MPCM slurries and PCM emulsions. Among other factors such as inlet temperature and flow rate of water through the exchanger tubes, stirring speed in the storage tank had a significant effect on the heat transfer inside the PCM-based fluids as well as the charging performance as a whole. In the present study, however, because heat exchange mainly occurred between the cooling tank and the PCM nano-emulsion in the system, mixing condition in the storage tank had little effect on the charging rate as shown in Fig. 5b. Moreover, with the direct transportation of the emulsion for charging, this system can achieve a faster charging rate and a higher thermal charging efficiency than other TES systems.

Table 3 presents the volumetric thermal storage capacity $E_{V,c}$ at various charging flow rates, and stirring speeds and the comparison with water in the range of 5–20 °C. The theoretical $E_{V,c}$ of water was 63 MJ/m^3, while a larger $E_{V,c}$ was attained for the PCM emulsion

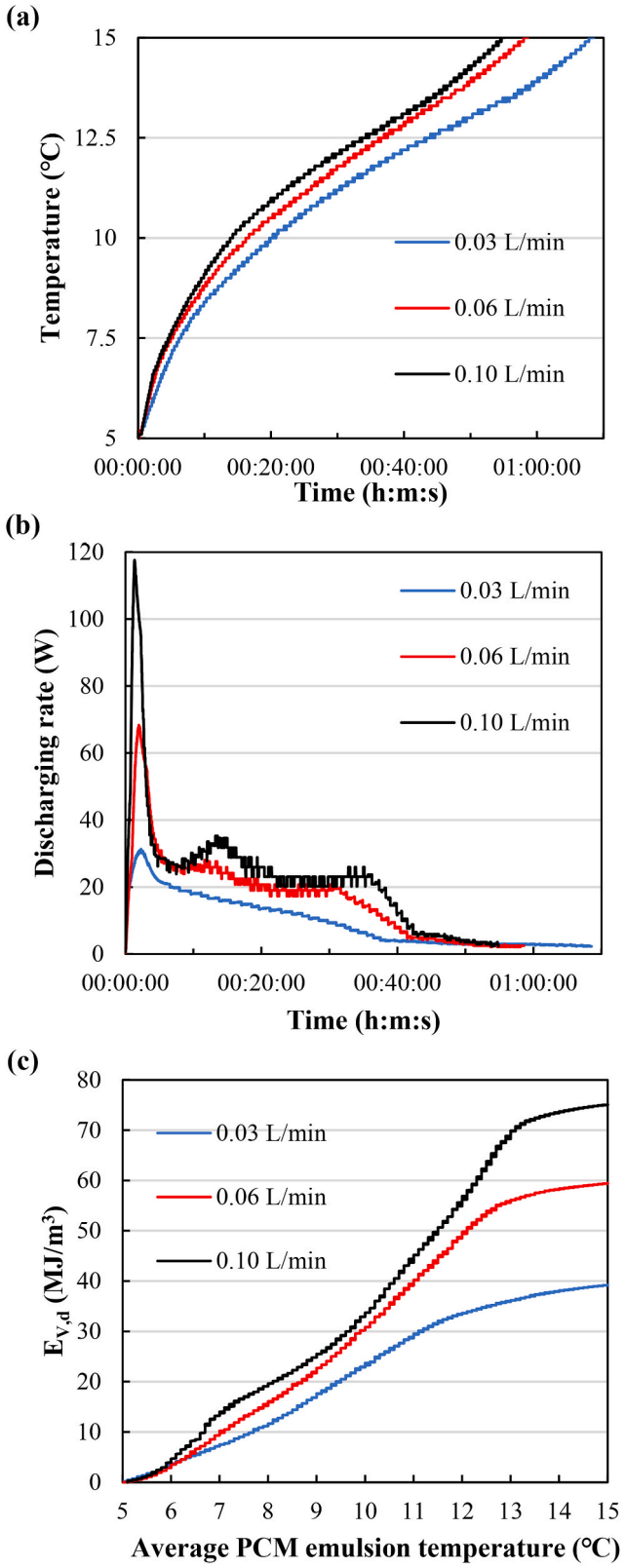

Fig. 6. The discharging process of PCM nano-emulsion with different flow rates at 700 rpm stirring: (a) average emulsion temperature in the storage tank; (b) discharging rate curves; (c) volumetric thermal storage capacity.

due to the higher latent heat storage capacity. As mentioned above, the stirring speed was less important than flow rate with a minor difference in $E_{V,c}$ after 30 min of charging. At a flow rate of 0.12 L/min and stirring speed of 1100 rpm, $E_{V,c}$ of the emulsion was 1.5 times higher than that of water, implying that the storage tank size can be dramatically reduced.

4.5. Discharging performance of PCM nano-emulsion

The discharging performance of PCM nano-emulsion in the system was further evaluated at various flow rates and 700 rpm stirring speed (Fig. 6). As shown in Fig. 6a, less time was needed at a higher flow rate to raise the temperature from 5 to 15 °C. Consequently, the shortest time was about 54 min at 0.10 L/min, which was similar to the charging process. The discharging time was increased by only 4 min from 54 min to 58 min as the flow rate was decreased from 0.10 L/min to 0.06 mL/min but increased more notably from 58 to 68 min with the flow rate from 0.06 mL/min to 0.03 L/min. Likewise, the corresponding discharging rate also decreased with the decrease of flow rate from 0.10 mL/min to 0.03 mL/min (Fig. 6b). Similar to the results with water, the time interval of the emulsion circulating in the system led to the sharp increase of discharging rate at the very beginning. In the later period, the higher charging rate was higher at a higher flow rate. Additionally, the discharging rate of the emulsion at the same flow rate such as 0.10 L/min was slightly higher than that of water.

Fig. 6c shows the discharging volumetric thermal storage capacity $E_{V,d}$ versus the average emulsion temperature in the storage tank during the discharging process derived from Eq. (6). As the flow rate was increased, the cooling energy released through the cooling panel increased gradually. Specifically, $E_{V,d}$ increased from 39.15 MJ/m^3 at 0.03 L/min to 59.39 at 0.06, and to 75.01 MJ/m^3 at 0.10 L/min. Therefore, the highest efficiency of cooling energy release was about 79% of the cooling energy storage. Considering the heat loss with the plastic tubing, this result implies that the direct transportation of the emulsion to the site of heat exchange can release most of the cooling energy as expected. This is a chief advantage of the system. It should also be noted that the slowdown of $E_{V,d}$ was expected to occur at the endset melting temperature of 15 °C. However, $E_{V,d}$ was calculated by the inlet and outlet temperature of cooling panel (T_6 and T_7) with the average emulsion temperature in the storage tank as the horizontal axis in Fig. 6c. Therefore, the slowdown point was closer to 15 °C at the higher flow rate with less heat loss from the plastic tubing before entering the cooling panel.

5. Conclusions

In this study, a PCM nano-emulsion was evaluated of its performance for cooling energy storage in a simple and small-scale tubular heat exchanger system. Of the two operating variables tested, the volumetric flow rate of emulsion circulating through the system was more significant than the stirring speed (mixing condition) in the emulsion storage tank. Overall, the charging and discharging performance with the PCM emulsion were all much better than those of water, e.g., up to 50% higher energy charging storage capacity in the temperature range of 5–20 °C. During the discharging process, 79% cooling energy could be released through the cooling panels. The PCM nano-emulsion remained stable throughout the test period and no pipeline blockage. Further study is underway to evaluate the thermal storage performance of the PCM emulsion in a larger TES system with a total emulsion volume of 55–60 L for potential application.

Author contributions

Liu Liu: Methodology; Investigation; Visualization; Writing-original draft.
Jing Li: Methodology; Investigation; Visualization.
Jianlei Niu: Supervision; Resources.
Jian-Yong Wu: Conceptualization; Project administration; Supervision; Writing-review & editing.

Declaration of competing interest

The authors declare that they have no known competing financial interests or personal relationships that could have appeared to influence the work reported in this paper.

Acknowledgments

This work was supported financially by the Environment and Conservation Fund (ECF Project 53/2018), the Research Grant Council of the Hong Kong SAR Government through General Research Fund (PolyU152707/16E), and by the Hong Kong Polytechnic University.

References

[1] D. Zhou, C.Y. Zhao, Y. Tian, Review on thermal energy storage with phase change materials (PCMs) in building applications, Appl. Energy 92 (2012) 593–605.
[2] F. Souayfane, F. Fardoun, P.-H. Biwole, Phase change materials (PCM) for cooling applications in buildings: a review, Energy Build. 129 (2016) 396–431.
[3] Z.A. Qureshi, H.M. Ali, S. Khushnood, Recent advances on thermal conductivity enhancement of phase change materials for energy storage system: a review, Int. J. Heat Mass Tran. 127 (2018) 838–856.
[4] N. Zhu, S. Li, P. Hu, S. Wei, R. Deng, F. Lei, A review on applications of shape-stabilized phase change materials embedded in building enclosure in recent ten years, Sustainable Cities and Society 43 (2018) 251–264.

[5] S. Nižetić, M. Jurčević, M. Arıcı, A.V. Arasu, G. Xie, Nano-enhanced phase change materials and fluids in energy applications: a review, Renew. Sustain. Energy Rev. 129 (2020) 109931.
[6] X. Huang, C. Zhu, Y. Lin, G. Fang, Thermal properties and applications of microencapsulated PCM for thermal energy storage: a review, Appl. Therm. Eng. 147 (2019) 841–855.
[7] Y. Fang, H. Xu, Y. Miao, Z. Bai, J. Niu, S. Deng, Experimental study of storage capacity and discharging rate of latent heat thermal energy storage units, Appl. Energy 275 (2020) 115325.
[8] F. Wang, W. Lin, Z. Ling, X. Fang, A comprehensive review on phase change material emulsions: fabrication, characteristics, and heat transfer performance, Sol. Energy Mater. Sol. Cell. 191 (2019) 218–234.
[9] F. Ma, P. Zhang, A review of thermo-fluidic performance and application of shellless phase change slurry: Part 2 – flow and heat transfer characteristics, Energy 192 (2020) 116602.
[10] F. Ran, Y. Chen, R. Cong, G. Fang, Flow and heat transfer characteristics of microencapsulated phase change slurry in thermal energy systems: a review, Renew. Sustain. Energy Rev. 134 (2020) 110101.
[11] L. Chai, R. Shaukat, L. Wang, H.S. Wang, A review on heat transfer and hydrodynamic characteristics of nano/microencapsulated phase change slurry (N/MPCS) in mini/microchannel heat sinks, Appl. Therm. Eng. 135 (2018) 334–349.
[12] B.M. Diaconu, S. Varga, A.C. Oliveira, Experimental study of natural convection heat transfer in a microencapsulated phase change material slurry, Energy 35 (2010) 2688–2693.
[13] M.J. Huang, P.C. Eames, S. McCormack, P. Griffiths, N.J. Hewitt, Microencapsulated phase change slurries for thermal energy storage in a residential solar energy system, Renew. Energy 36 (2011) 2932–2939.
[14] S. Zhang, J. Niu, Two performance indices of TES apparatus: comparison of MPCM slurry vs. stratified water storage tank, Energy Build. 127 (2016) 512–520.
[15] H. Xu, Y. Miao, N. Wang, Z. Qu, X. Wang, Experimental investigations of heat transfer characteristics of MPCM during charging, Appl. Therm. Eng. 144 (2018) 721–725.
[16] F. Ma, J. Chen, P. Zhang, Experimental study of the hydraulic and thermal performances of nano-sized phase change emulsion in horizontal mini-tubes, Energy 149 (2018) 944–953.
[17] T. Morimoto, H. Kumano, Flow and heat transfer characteristics of phase change emulsions in a circular tube: Part 1. Laminar flow, Int. J. Heat Mass Tran. 117 (2018) 887–895.
[18] T. Morimoto, H. Kumano, Flow and heat transfer characteristics of phase change emulsions in a circular tube: Part 2. Turbulent flow, Int. J. Heat Mass Tran. 117 (2018) 903–911.
[19] M. Delgado, A. Lázaro, J. Mazo, C. Peñalosa, P. Dolado, B. Zalba, Experimental analysis of a low cost phase change material emulsion for its use as thermal storage system, Energy Convers. Manag. 106 (2015) 201–212.
[20] M. Delgado, A. Lázaro, J. Mazo, C. Peñalosa, J.M. Marín, B. Zalba, Experimental analysis of a coiled stirred tank containing a low cost PCM emulsion as a thermal energy storage system, Energy 138 (2017) 590–601.
[21] L. Liu, J. Niu, J.-Y. Wu, Formulation of highly stable PCM nano-emulsions with reduced supercooling for thermal energy storage using surfactant mixtures, Sol. Energy Mater. Sol. Cell. 223 (2021) 110983.
[22] X. Wang, J. Niu, Performance of cooled-ceiling operating with MPCM slurry, Energy Convers. Manag. 50 (2009) 583–591.
[23] R.J. Moffat, Describing the uncertainties in experimental results, Exp. Therm. Fluid Sci. 1 (1988) 3–17.
[24] S. Zhang, J. Niu, Experimental investigation of effects of supercooling on microencapsulated phase-change material (MPCM) slurry thermal storage capacities, Sol. Energy Mater. Sol. Cell. 94 (2010) 1038–1048.